PREDICTION OF 3D FLOW FIELD AND LOCAL SCOURING AROUND SPUR DYKES

Hao ZHANG[1], Hajime NAKAGAWA[2], Taisuke ISHIGAKI[3] and Yasunori MUTO[4]

[1]Student Member of JSCE, Doctoral Student, Graduate School of Eng., Kyoto University
[2]Member of JSCE, Dr. of Eng., Professor, Disaster Prevention Research Institute, Kyoto University
[3]Member of JSCE, Dr. of Eng., Associate Professor, Disaster Prevention Research Institute, Kyoto University
[4]Member of JSCE, Dr. of Eng., Disaster Prevention Research Institute, Kyoto University
(Shimomisu, Yoko-oji, Fushimi-ku, Kyoto 612-8235, Japan)

Numerical investigation of the 3D flow and sediment transport around a series of non-submerged spur dykes has been presented. The complex velocity field and bed shear stress are predicted by the widely used k-ε model in combination with the wall function approach. Coupling the mass conservative equation of the sediment with an empirical formula for the bed load transport, a scour model has been put forward. The effect of the local bed slope is taken into account by correcting the threshold condition for the sediment entrainment and incorporating the particle gravity as a part of the effective shear stress. A sand slide process is introduced to avoid the excess slope over the angle of sediment repose. The model result has been compared with the laboratorial experiment. It is shown that both the velocity field and the local scouring predicted by the current model are in reasonable agreement with those of the experiment.

Key Words : *3D flow, spur dyke, k-ε model, local scouring*

1. INTRODUCTION

Spur dykes are one of the most commonly used hydraulic structures for river training and river restoration. In order to increase the efficiency and enlarge the improved stretch of the river system, spur dykes are generally designed and organized in sequences. Single spur dykes can change only the local river conditions, so they are hardly found in the engineering construction. As spur dykes act like blockages to the river flow, the flow separation will be obviously observed at the heads of the spur dykes. In the embayments formed by the consecutive spur dykes, secondary flows and sediment transport present quite challenging and interesting problems for engineers and researchers.

A vast number of experiments have been carried out in laboratorial flumes with single or groups of spur-dyke-like structures during the last decades. e.g. Melville [1], Ishigaki et al.[2] and Uijttewaal et al.[3] These studies provide a substantial collection of data and help to further the understanding of the behavior of spur-dyke-like structures. But the drawbacks of experimental methods are also well documented. For example, the high cost of physical models, the idealized flow and sediment conditions, the simplified study domain geometry, etc. Moreover, as the result is usually experiment dependent, the relationship or empirical formula concluded from the experiment analyses have to be prudently applied to field situations.

A more cost-effective alternative, namely, the numerical method, has achieved great development in the past several years, e.g. the quasi-3D numerical simulation by Muneta and Shimizu [4], the 3D calculation performed by Kawaguchi et al.[5] A well-established numerical model can resolve the evolution process of the 3D flow field and the 3D topography of the local scour hole, which is of significant meaning for the engineering practice.

Although numerical investigation of the 3D flow and/or sediment transport is attracting more and more attention, most of the published papers are limited to the flow passing over a fixed bed or scouring around an individual spur-dyke-like structure. For instance, in order to simulate the flow separation and vortex shedding from the tip of two skewed spur dykes, Kimura et al. developed a

non-linear k-ε model [6]. The computed 3D flow field was reported to be very similar to the PIV (Particle Image Velocimetry) measurements. Omitting the transient term, Olsen and Melaaen computed the scour hole around a cylinder by solving the 3D RANS (Reynolds-Averaged Navier-Stokes) equation with the k-ε model for the Reynolds stresses and the convection-diffusion equation for the sediment transport [7]. The computational result was found to be in agreement with the observed data after a 12-hour run. Peng et al. calculated the flow field around a spur dyke with a modified k-ε turbulence model [8]. And the scour hole was simulated with the bed load transport formula proposed by Meyer-Peter and Muller. They got a slightly different scour pattern from the experiment when the equilibrium depth was reached. According to the previous researches, the techniques of turbulence modeling are relatively well-developed, but simulation of the sediment behavior is still a major limitation for further applications of such morphological models.

This paper examines the flow field around a series of spur dykes with a 3D k-ε turbulence model. The local scouring is assumed to take place in the form of bed load transport and modeled with the Ashida-Michiue formula [9]. The bed slope effect is taken into account by correcting the threshold condition of the sediment entrainment and including the gravitational force in the effective shear stress acting on the particles. Furthermore, the excess of the bed slope over the angle of sediment repose is avoided by introducing a sand slide algorithm. The computation is performed under the experimental conditions in the laboratorial test by Muto et al.[10] and the model verification is carried out through the comparison with the measured data.

2.MODEL DESCRIPTION

(1) Flow field

The 3D RANS equations and the continuity equation expressed in a Cartesian coordinate system with the Einstein summation convention are as follows.

Momentum equation

$$\frac{\partial u_i}{\partial t}+u_j\frac{\partial u_i}{\partial x_j}=f_i-\frac{1}{\rho}\frac{\partial p}{\partial x_i}+\nu\frac{\partial^2 u_i}{\partial x_j\partial x_j}+\frac{1}{\rho}\frac{\partial \tau_{ij}}{\partial x_j} \qquad (1)$$

Continuity equation

$$\frac{\partial u_i}{\partial x_i}=0 \qquad (2)$$

where u_i= averaged velocity field; x_i= Cartesian coordinate component; t= time; ρ = density of the fluid; f_i= body force; p= averaged pressure; ν= molecular kinematic viscosity of the fluid; $\tau_{ij}=-\rho\overline{u_i'u_j'}$, are defined as the Reynolds stress tensors, and u_i' is the fluctuating velocity field.

The transport equations for the turbulence kinetic energy k and its dissipation rate ε read

$$\begin{aligned}\frac{\partial k}{\partial t}+u_j\frac{\partial k}{\partial x_j}&=\frac{\partial}{\partial x_j}\left[\left(\nu+\frac{\nu_t}{\sigma_k}\right)\frac{\partial k}{\partial x_j}\right]+G-\varepsilon\\ \frac{\partial \varepsilon}{\partial t}+u_j\frac{\partial \varepsilon}{\partial x_j}&=\frac{\partial}{\partial x_j}\left[\left(\nu+\frac{\nu_t}{\sigma_\varepsilon}\right)\frac{\partial \varepsilon}{\partial x_j}\right]+\left(C_{1\varepsilon}G-C_{2\varepsilon}\varepsilon\right)\frac{\varepsilon}{k}\end{aligned} \qquad (3)$$

where G= the rate of production of turbulence kinetic energy; the eddy viscosity $\nu_t=C_\mu k^2/\varepsilon$, and in a standard k-ε model, the following coefficients are generally used:

C_μ=0.09, σ_k=1.0, σ_ε=1.3, $C_{1\varepsilon}$=1.44, $C_{2\varepsilon}$=1.92

(2) Sediment modeling

a) Bed evolution

The scour hole is generated by the sediment transport. It is usually modeled by solving the sediment continuity equation

$$(1-\lambda)\frac{\partial z_b}{\partial t}+\left[\frac{\partial q_{bx}}{\partial x}+\frac{\partial q_{by}}{\partial y}\right]=0 \qquad (4)$$

where z_b= river bed elevation; λ = porosity of sediment; q_{bx}, q_{by} = bed load transport rate in x and y direction, respectively.

If the sediment particles are relatively coarse, they mainly move as bed load, i.e. they basically move by rolling, sliding or jumping along the bed. Among numerous formulae, the approach for bed load transport rate proposed by Ashida and Michiue is adopted here, which has the form as below.

$$\frac{q_b}{\sqrt{(s-1)gd^3}}=17\tau_{*e}^{3/2}\left(1-\sqrt{\frac{\tau_{*c}}{\tau_*}}\right)\left(1-\frac{\tau_{*c}}{\tau_*}\right) \qquad (5)$$

where q_b= bed load discharge per unit width; s= specific gravity of sediment; g= gravitational acceleration; d= diameter of sediment; $\tau_{*e}, \tau_{*c}, \tau_*$ = dimensionless effective shear stress, critical shear stress and shear stress, respectively.

b) Local bed effect

Due to the sediment transport, the bed topography becomes very complex. The bed slope effect is no longer negligible in the calculation of

the sediment transport rate. It is taken into account by correcting the critical condition of the particles incipient motion and including the gravitational component as a part of the effective shear stress.

A particle resting on a local bed surface with a normal direction (α, β, γ) will be set in motion if the resulted driving force is larger than the stabilizing force. Due to the slope, the direction of the particle movement does not coincide with the flow any more, but is related to the immersed weight of the particle **W** and the fluid force **F** acting on the particle. Writing the fluid force as the multiplication of its magnitude and direction vector, i.e.

$$\mathbf{F} = F\left(f_x\mathbf{i} + f_y\mathbf{j} + f_z\mathbf{k}\right) \tag{6}$$

in which F= magnitude of the fluid force **F**; **i, j, k**= the unit vector in x, y, z direction, respectively and f_x, f_y, f_z= direction cosines of the fluid force **F**, the resulted driving force $\mathbf{F_R}$ has the form

$$\mathbf{F_R} = \left(W\cos\gamma\cos\alpha + f_x F\right)\mathbf{i} + \left(W\cos\gamma\cos\beta + f_y F\right)\mathbf{j} + \left(-W\sin^2\gamma + f_z F\right)\mathbf{k} \tag{7}$$

where W=magnitude of the immersed weight **W**, and the magnitude of the stabilizing force F_S is

$$F_S = -W\cos\gamma\tan\phi \tag{8}$$

where ϕ = the angle of sediment repose underwater.

Comparing the forces above with those on a horizontal bed, the critical fluid force (here expressed in terms of the shear stress) on a sloping bed has the following form.

$$\tau_c = K\tau_{c0} \tag{9}$$

in which τ_c, τ_{c0} = the critical shear stress for a sloping bed and a horizontal bed, respectively; the bed slope factor K is expressed by

$$K = \frac{\sqrt{m^2 - \sin^2\gamma + \cos^2\gamma\tan^2\phi} - m}{\tan\phi} \tag{10}$$

where $m = f_x\cos\gamma\cos\alpha + f_y\cos\gamma\cos\beta - f_z\sin^2\gamma$

Liu[11] also theoretically derived a bed slope factor by constructing two curvilinear coordinate systems. But the resulted formula was too complex to ensure a numerical implementation. In the current model, two assumptions have been made: the ratio of the lift force to the particle weight underwater is small and the Reynolds number is relatively high. With this simplification, the method is applicable.

It is also important to determine the bed load components in the Cartesian coordinate system, which necessitates the evaluation of the direction of sediment transport. It is herein assumed that the direction of the sediment movement follows the direction of the resulted driving force. Then the sediment transport rate in different directions is explicitly acquired.

In some literatures such as van Rijn's publication [12], the bed slope factor has been divided into a longitudinal slope factor and a transverse slope factor. According to the authors' numerical experiments, this kind of treatment seems not very suitable for a 3D calculation. In addition, it can be verified that either the longitudinal slope factor or the transverse slope factor suggested by van Rijn is a special case of Eq. 10.

c) Sand slide

During the bed evolution, the bed slope may increase to a level larger than the angle of repose, in particular around the scour holes. This phenomenon cannot occur, or it is not stable in the actual case. In the numerical simulation, an indicator and a sand slide process are introduced to avoid its occurrence.

A moving unstructured 3D mesh has been adopted in this study. During the calculation, the mesh changes with the bed variation. On the riverbed, the topography of the surface mesh (all the mesh elements are assumed to be planar polygons) is shown in Fig.1. Each time before adjusting the mesh, the program checks all the mesh nodes and corresponding neighbors on the bed surface.

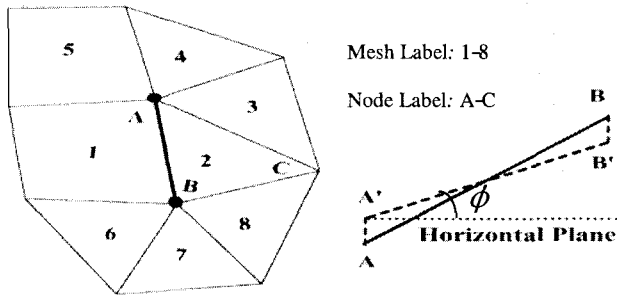

Fig.1 Sand slide process

For example, an angle steeper than the angle of repose (see Fig.1) has been detected connecting node ***A*** (x_A, y_A, z_A) and node ***B*** (x_B, y_B, z_B). If node ***B*** is higher, it should be lowered vertically to node ***B'***, and node ***A*** should increase a distance to node ***A'*** at the same time. Finally the angle connecting ***A*** and ***B*** is equal to the angle of repose, i.e.

$$\left(z_B - \delta z_B\right) - \left(z_A + \delta z_A\right) = \tan\phi\sqrt{\left(x_B - x_A\right)^2 + \left(y_B - y_A\right)^2} \tag{11}$$

in which δz_A, δz_B = vertical change amount for

node ***A*** and node ***B***, respectively.

On the other hand, the sediment conservation should be ensured amidst the adjustment, it results in

$$(S_1+S_2+S_3+S_4+S_5)\delta z_A=(S_6+S_7+S_8+S_2+S_1)\delta z_B \quad (12)$$

where S= projected area of the bed surface in the x-y plane.

From Eq.11 and Eq.12, the new position of node ***A*** and node ***B*** can be determined. For each node on the riverbed, the process is repeated. As the change of one node has an influence on all the angles connecting the node and its neighboring nodes, new scans and possible adjustments are needed until all the angles are not greater than the angle of repose.

(3) Solution procedure

The governing equations for the turbulence are discretized by a cell-centered FVM (Finite Volume Method). A moving unstructured mesh is adopted so that the model can be extended to actual rivers without any *ad hoc* treatment. A detailed description of the numerical scheme and boundary conditions was given in another paper written by the authors.[13)]

Based on the shear stress calculated from the turbulence model at one time step, the sediment erosion and deposition can be evaluated with the methods proposed in the previous contexts. The riverbed elevation is then adjusted. A new mesh is generated based on the new bed geometry and the calculation time is forward. If the maximum bed change is larger than a specific number (8% of the water depth in this study), a new flow field and therefore a new shear stress is calculated with the new mesh. This procedure is repeated until the maximum bed variation per second is so small (less than 10^{-4} cm/s in this study) that it can be considered as an equilibrium condition.

3. EXPERIMENT AND COMPUTATION CONDITIONS

The laboratorial experiment was conducted in a straight compound channel with a slope 1/700 as shown in Fig. 2. Removing some parts of the flood plain area, 9 consecutive spur dykes have been set up along the channel. The initial riverbed is covered by 10cm-thick artificial spherical sands with a mean diameter of d= 1.34mm. The density of the sediment particle is 2.24 g/cm^3, which is a little lighter than the natural sand. The experimental conditions are given in Tab.1.

After a continuous running of 24 hours, the bed seems to be unchanged and it is assumed as an equilibrium state. The riverbed deformation was then measured with a laser sensor after the flume has been completely drained out. Cements were utilized to fix the final riverbed for the measurement of the velocity field. An I-shape and an L-shape electromagnetic velocimeters were employed to measure the flow velocities.

Table 1 Hydraulic condition for the experiment

Discharge	Water Depth	Mean Velocity	Re. Number	Fr. Number
8.23 l/s	4.30 cm	28.57 cm/s	12,285	0.44

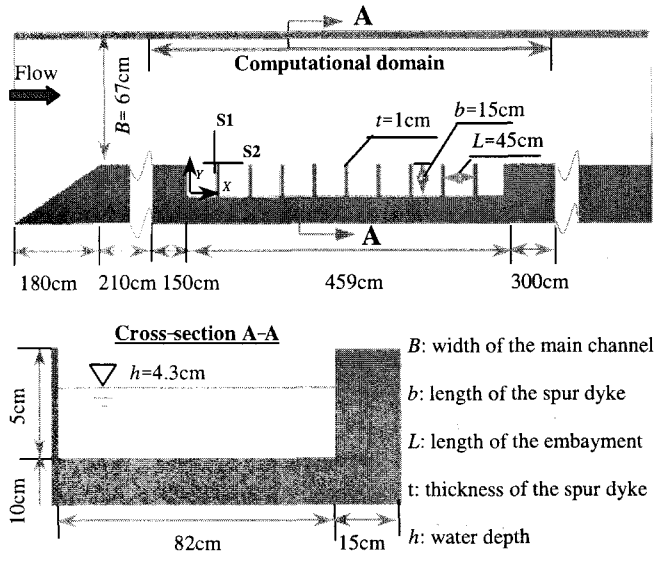

Fig.2 Experiment set-up (top view,top;side veiw,bottom,not to scale)

Considering the computational convenience, the computed domain does not completely coincide with the experimental geometry. It begins 10*b* (i.e. 150cm) upstream from the first embayment and extends to 20*b* (i.e. 300cm) downstream from the last embayment. As is seen in Fig. 2, there is a 180cm gradually narrowing stretch in the upstream area in this experiment. It intends to have some influence on the approaching flow. However, it is assumed at the current stage that the turbulent flow has been fully developed in the main stream. This assumption might have some impacts on the values of the simulated result, but it does not affect the generality of the conclusion.

With the adopted geometry, a total number of 14,196 hexahedral mesh has been used in this test case. The initial conditions are obtained by carrying out a steady-state calculation on the flat bed. After that, the sediment is exposed to the flow and subject to move until the equilibrium state.

4. RESULTS AND DISCUSSIONS

(1) Bed variation

The comparison of the final riverbed variation around the first four embayments is shown in Fig.3.

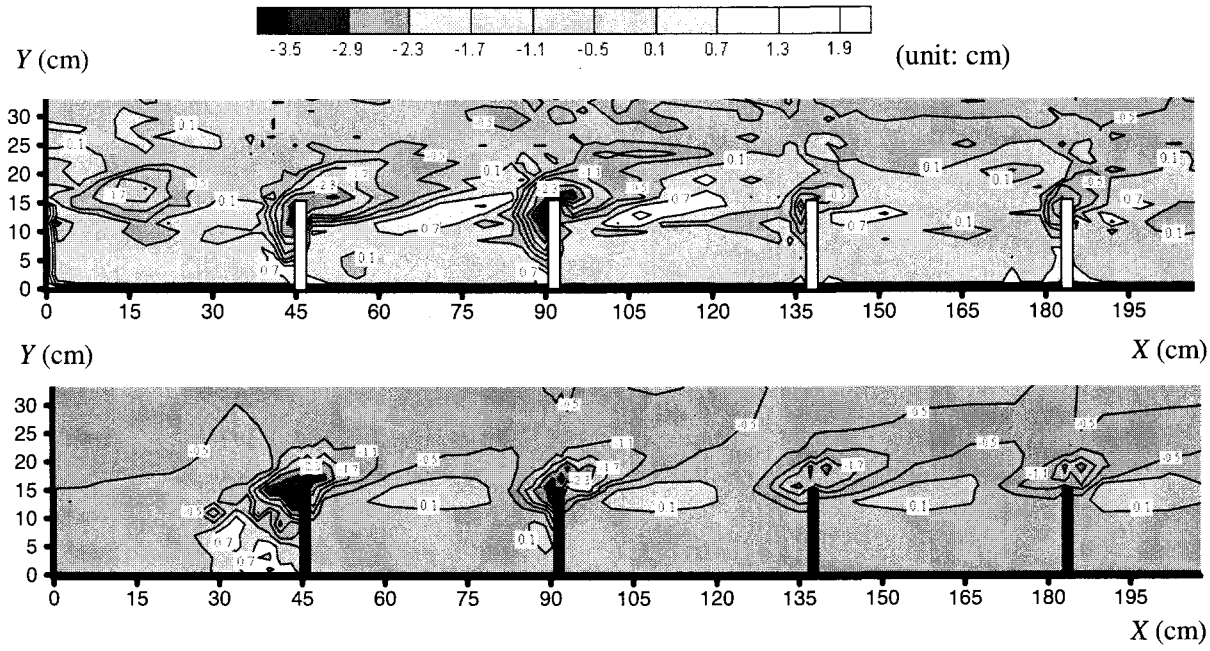

Fig.3 Final bed variation δz_b (Experiment: top; Computation: bottom)

There are some differences, but both the experiment and simulation exhibit that local scouring occurs at the toes of all the spur dykes. Around the first two spur dykes, the scour holes are quite remarkable. Consequently, the toe protection becomes a great consideration from the standpoint of structure design. The depth of the scour hole is very small at the third spur dyke, and so are all the others.

The final bed variation δz_b from the initial flat bed normalized by the maximum scour hole depth H_{max} along two representative sections (see Fig.2: Section S1, i.e. X/L=1 and Section S2, i.e. Y/b=1) are given in Fig.4. It illustrates the longitudinal and transverse scour hole profiles around the first spur dyke. The computational result in these two sections is quite similar to the experimental data.

In the experimental result, the deepest scour hole around the first spur dyke is about 3.69cm, and the second one is 4.37cm. However, as shown in Fig.3, the deepest scour hole calculated is at the toe of the first spur dyke (4.03cm) and the second one has a depth of around 3.68cm. This might be attributed to the difference between the experimental condition and the computational condition. Due to the narrowing stretch upstream, the fully developed turbulent flow was not achieved at the spur dyke stretch, but this effect has been omitted in the turbulence modeling. In the first embayment, the deposition pattern is a little different from the experiment. Near the channel bank, the bed is almost unchanged, but a large area of deposition has been calculated. It demonstrates that the shear stress might have been over-estimated by the k- ε model.

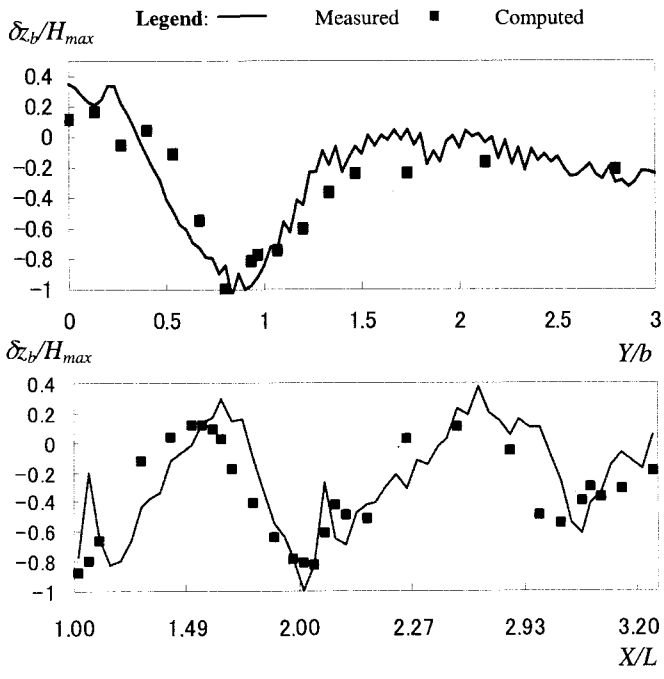

Fig.4 Scour hole profile (Section S1: top; Section S2: bottom)

(2) Flow field

The comparison of the stream-wise velocity (u, v) around the first three spur dykes at depth z=2.3cm from the datum level is shown in Fig.5. The similarity of the flow pattern between the measurement and the computation is evident.

The flow diverts at the heads of the spur dykes, which results in extreme lateral velocity gradient. The longitudinal velocity is still dominated in the main channel area. In the embayment area, horizontal vertices are obviously observed, but the

measured velocity seems to be a little larger than the computed result. In-between the embayment and the main channel area there is a junction zone where mass and momentum exchanges occur. The lateral velocity in the junction zone is also observed to be a bit under-estimated. The simplification of the input flow and the error introduced by the calculated final bed topography might be responsible for this discrepancy.

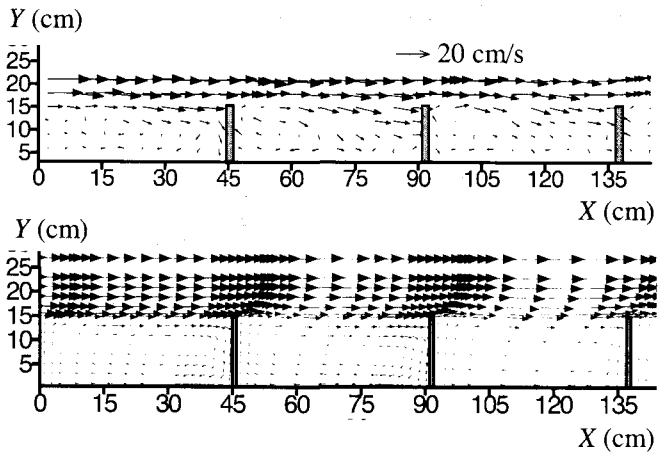

Fig.5 Stream-wise velocity profile (u, v) at depth z= 2.3cm (Experiment: top; Computation: bottom)

Furthermore, the drawbacks of the standard k-ε model also deserve attention as has mentioned before. In this experiment, the aspect ratio is L/b=3. With this aspect ratio, it has been verified that a more elaborate model will lead to a better result, for instance, a non-linear k-ε model [13]. It will be included in the future research.

5. CONCLUSIONS

A morphological model has been proposed to predict the 3D flow and sediment transport around a series of non-submerged spur dykes. Due to the interaction between the flow field and the bed morphology, the movement of sediment becomes much sophisticated. Hence, the modeling of sediment behavior has been emphasized.

By examining the forces acting on an individual particle, the threshold condition and effective shear stress for the sediment transport on a sloping bed have been analyzed. With some treatments, the bed load transport rate formulae for the horizontal bed can be easily extended to the sloping bed. A sand slide algorithm is introduced to avoid the unreasonably steep slope possibly produced by the numerical procedure. It guarantees that the bed slope is not greater than the angle of repose as well as ensures that the sediment conservativeness is maintained. Although the test mesh is a bit coarse and there are some simplifications between the experimental and computational conditions, the velocity field and scour pattern resulted from the numerical model are in reasonable agreement with those of the experiment. This demonstrates that the methodology proposed in this study is applicable.

ACKNOWLEDGMENT: This work is sponsored by the Monbukagakusho (MEXT, Japan) under Grant No.14350265.

REFERENCES

1) Melville, B. W.: Local scour at bridge abutments, *Journal of Hydraulic Engineering, ASCE*, Vol.118 (4), pp.615-631, 1992

2) Ishigaki, T., Baba, Y. and Muto, Y.: Vortex motion around a plate with footing in open channel flow and its effect on local scouring, *Advances in Hydro-Science and -Engineering*, Vol.4, pp.169-176, Seoul, 2000

3) Uijttewaal, W.S.J., Lehmann, D. and van Mazijk, A: Exchange processes between a river and its groyne fileds: model experiments, *Journal of Hydraulic Engineering, ASCE*, Vol. 127(11), pp. 928-936, 2001

4) Muneta, N. and Shimizu, Y.: Numerical analysis model with spur-dike considering the vertical flow velocity distribution, *J. of Hydraulic, Coastal & Environmental Engineering, JSCE*, No.497/ II -28, pp.31-39, 1994 (in Japanese)

5) Kawaguchi, H., Fukuoka, S. and Watanabe, A.: Flow and hydrodynamic force distributions of submersed groins for different groin angles, *Annual Journal of Hydraulic Engineering, JSCE*, Vol.48, pp.137-142, 2004 (in Japanese)

6) Kimura, I, Hosoda, T. and Onda, S.: Prediction of 3D flow structures around skewed spur dikes by means of a non-linear k-ε model, *River Flow 2002*, Bousmar D. and Zech, Y. (Eds.), Balkema, Vol.1, pp.65-73, 2002

7) Olsen, N. R. B. and Melaaen, M. C: Three-dimensional calculation of scour around cylinders, *Journal of Hydraulic Engineering, ASCE*, Vol. 119(9), pp. 1048-1054, 1993

8) Peng, J., Tamai, N, Kawahara, Y. and Huang, G.W.: Numerical modeling of local scour around spur dykes, *Proceedings of 28th IAHR Congress*,1998 (CDs)

9) Ashida, K. and Michiue, M.: Studies on bed load transportation for nonuniform sediment and river bed variation. *Disaster Prevention Research Institute Annuals, Kyoto Univ.*, No.14B, 1971. (in Japanese)

10) Muto, Y., Kitamura, K., Khaleduzzaman, A.T.M. and Nakagawa, H.: Flow and bed topography around impermeable spur dykes, *Advances in River Engineering, JSCE*, Vol.9, 2003 (in Japanese)

11) Liu, B.Y.: *Study on Sediment Transport and Bed Evolution in Compound Channels*, Ph.D thesis, Kyoto Univ., 1991

12) Van Rijn, L. C.: *Principles of Sediment Transport in Rivers, Estuaries and Coastal Seas*, AQUA Publications, Amsterdam, The Netherlands, 1993

13) Nakagawa, H., Zhang, H., Ishigaki, T. and Muto, Y.: Prediction of 3D flow field with non-linear k-ε model based on unstructured mesh, *Journal of Applied Mechanics, JSCE*, Vol.7 (2), pp.1077-1088, 2004

(Received September 30, 2004)